

Monitoring surface structure and interfacial properties via second harmonic generation

J. M. Robinson, H. M. Rojhtantalab, V. L. Shannon, D. A. Koos, and G. L. Richmond

Chemistry Department, University of Oregon, Eugene, OR 97403 USA

Abstract - Several studies are presented which demonstrate the application of SHG to the study of interfaces. Results are reported for experiments correlating the SH signal from the electrochemical silver/aqueous electrolyte junction with the electrostatics of the interface as simultaneously monitored by differential capacitance. For related studies, *in situ* measurements of the surface morphology and structural symmetry of immersed Ag(111) surfaces are presented. The third set of experiments examines the surface SHG from several technologically important semiconducting chalcogenide materials under ambient conditions.

INTRODUCTION

The nonlinear optical process, second harmonic generation (SHG), can serve as a powerful means of studying interfacial properties. SHG is electric dipole forbidden in bulk centrosymmetric media, but is allowed at the interface between two such media, where the inversion symmetry is broken (ref. 1). This property can be exploited to elucidate the equilibrium structure of the components of the junction between two dense media. Another potentially valuable application of SHG is in the measurement of the ultrafast chemical and physical interactions occurring at the interface.

Recent studies using SHG have demonstrated the diversity of phenomena that can be probed (ref. 2). The systems investigated include solid/vacuum (ref. 3), liquid/vapor (ref. 4) and solid/liquid (ref. 5) junctions. The work reported here is a brief overview of several ongoing studies in our laboratory in this area. The first experiments to be described have been aimed at developing SHG as a quantitative probe of ionic adsorption at the electrochemical interface. The unique sensitivity of SHG to the electrostatic properties of the double layer has been demonstrated (refs. 6,7). The studies reported here provide a more detailed examination of this correspondence by coupling differential capacitance with the nonlinear optical technique.

The second set of experiments addresses a related subject pertaining to the immersed electrode surface. Crystal surface structure plays an important role in the chemical reactivity of the electrode surface. Unfortunately, good *in situ* probes of surface morphology do not exist. Although surface homogeneity may be indicated by classical electrochemical methods, such as cyclic voltammetry, these methods do not completely describe the electrode surface. Characterization in vacuum can verify the surface structure but provides no information about the changes that occur upon immersion in electrolyte. Scanning tunneling microscopy (STM) shows promise as an *in situ* probe; however, it is currently limited to static measurements on very small electrode areas (ref. 8). In this paper we report the first use of an optical technique for determining surface structure in solution. The results for silver single crystals demonstrate a remarkable sensitivity to surface ordering and symmetry.

These first two studies investigate the equilibrium properties of the electrochemical interface. Of equal importance is the application of SHG to dynamic measurements. Time resolved SHG measurements have the potential to probe kinetics and dynamics of interfacial processes on nanosecond and faster timescales. These processes include photocarrier generation and recombination as well as electron transfer reactions. In the third set of studies to be discussed, we have chosen to investigate the nonlinear optical properties of two types of chalcogenide materials, amorphous selenium and the transition metal dichalcogenides ZrSe₂ and WSe₂. Both types of materials are of technological interest due to their respective use in Xerography and photoelectrochemistry. The work described here comprises the preliminary ambient measurements of signal intensity and damage threshold under steady state conditions using both nanosecond and picosecond lasers and provides the foundation for time-resolved SHG experiments.

EXPERIMENTAL TECHNIQUES

Figure 1 shows the experimental apparatus for the investigation of the materials discussed here. The collimated p-polarized 1.06 μm light from a Q-switched Nd:YAG laser (10 nsec pulses at 10 Hz) impinges on the sample at approximately 45°. A cooled photomultiplier tube and gated electronics monitor the second harmonic (532 nm) light generated at the angle of specular reflectance following rejection of the fundamental beam by color filters and a monochromator. The SHG measurements of amorphous selenium films employ the focussed output of a cw mode-locked Nd:YAG laser (120 psec pulses at 82 MHz) and single photon counting in a similar configuration. Laser fluence is kept well below the damage threshold for each of the materials studied.

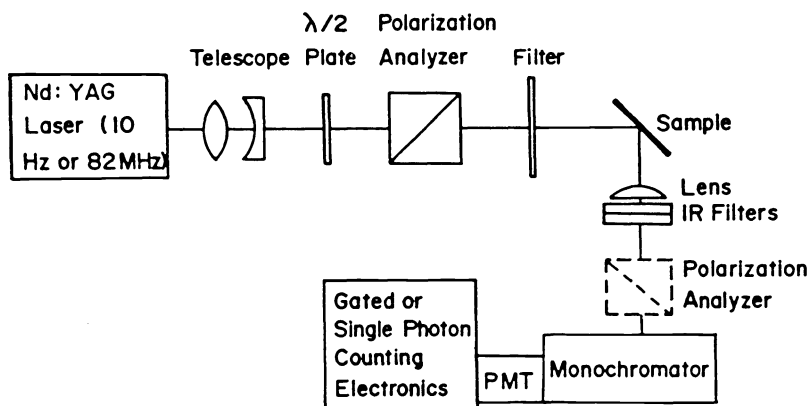


Fig. 1. Experimental apparatus for second harmonic generation.

The silver electrodes are mechanically polished to a mirror finish with 0.05 μm alumina grit and then electrochemically polished to remove any oxide layer (ref. 9). The amorphous selenium films are prepared by chemical vapor deposition onto quartz substrates, and the dichalcogenide single crystal surfaces are obtained by cleavage of the top layer from the sample. Differential capacitance versus potential is measured using a lock-in amplifier with an internal oscillator set at 57 Hz, 4 mV peak-to-peak AC amplitude and sweep rates of 2 to 5 mV/s. The surface morphology experiments are performed by rotating the silver electrode (0.75° per step) and measuring the p- and s-polarized SH signals for p-polarized input as a function of angle of rotation.

RESULTS AND DISCUSSION

SHG (second harmonic generation) and differential capacitance studies

Recent studies have shown SHG to be a useful probe of the metal/liquid double-layer structure (refs. 6,10,11). Early work on silver evaporated films in aqueous solutions of KCl by Lee *et al.* (ref. 12) suggested that the SH signal is quadratically related to the applied bias voltage. More recent work on polished silver single crystal surfaces (ref. 6) and silver thin films (ref. 7) applied Gauss' Law and suggested that, for simple adsorption of ions on the surface, the SH intensity is proportional to the square of the metal surface charge density. We have tested this model by comparing the SH intensity produced for polycrystalline smooth silver, potentiostated in different mixtures of NaCl-NaClO₄ electrolytes at constant ionic strength, with simultaneously measured differential capacitance data.

Second harmonic generation at an interface between two centrosymmetric media is proportional to the square of the nonlinear polarizability, $\vec{P}_{nl}(2\omega)$, of the interface. Under conditions where the electric dipole approximation holds, the nonlinear polarizability in an externally applied potential can be expressed as:

$$\vec{P}_{nl}(2\omega) = \vec{\chi}^{(2)}(2\omega) : \vec{E}(\omega) \vec{E}(\omega) + \vec{\chi}^{(3)}(2\omega) : \vec{E}_{dc} \vec{E}(\omega) \vec{E}(\omega) \quad (1)$$

where $\vec{\chi}^{(2)}$ and $\vec{\chi}^{(3)}$ are the second order and third order nonlinear susceptibility tensors which have contributions from both sides of the interface (ref. 13). Although $\vec{\chi}^{(3)}$ is

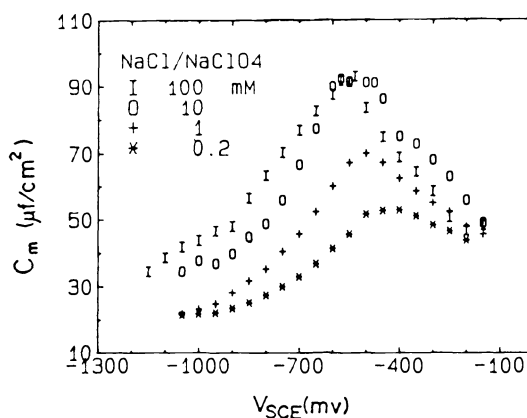


Fig. 2. Differential capacitance vs. electrode potential for electropolished polycrystalline silver in NaCl-NaClO₄ mixtures at ionic strength of 0.5 and chloride ion concentration of 0.2, 1.0, 10, and 100 mM.

several orders of magnitude smaller than $\chi^{\leftrightarrow(2)}$, the large electric field strength at the interface ($E_{dc} \cong 10^6$ V/cm) makes the third order term of comparable or greater magnitude. Assuming a flat surface, the electric field at the surface should be proportional to the surface charge density by Gauss' Law.

In Fig. 2 the differential capacitance curves, $C_m(E)$, are displayed for an electropolished polycrystalline silver electrode in different concentrations of NaCl at constant ionic strength of 0.5 using NaClO₄ as supporting electrolyte. Both in phase and quadrature components were used in measuring $C_m(E)$. The data were collected in both positive and negative directions in the ideally polarizable region, avoiding solvent reduction and metal oxidation. At very negative potentials, capacitance becomes almost independent of chloride ion concentration. As the potential becomes more positive, $C_m(E)$ increases progressively as a consequence of greater chloride specific adsorption. With increasing bulk concentration of chloride ion, its maximum value corresponding to half monolayer coverage moves cathodically.

What is the contribution of each side of the interface to the SH signal? As the interface is polarized, the charge density on the solution side of the interface, σ_s , increases and is distributed throughout the double layer. By electroneutrality, an equal and opposite amount of charge builds on the metal side. Therefore, σ_m is a measure of the excess charge density on the metal at a given potential brought about by adsorbing anions. Interfacial capacitance is defined as the ability of the interface to store charge in response to a change in potential:

$$C_m = (\delta\sigma_m / \delta E) \quad (2)$$

Thus, the magnitude of σ_m can be found by back integrating the $C_m(E)$ curves. In Fig. 3(a) the resultant σ_m^2 vs. E is shown for our $C_m(E)$ data. For comparison in Fig. 3(b) the SHG vs. potential is displayed for the same electrode. The SH adsorption profile in Fig. 3(b) shifts to more negative potential and its intensity increases with an increase in chloride bulk concentration. The results in Fig. 3 support the claim that the SH intensity generated at the silver-aqueous interface reflects the adsorption of anions to the metal surface and also demonstrate the correlation between σ_m^2 and the SH signal. The best fit occurs at the lower coverages with a deviation beyond -0.400 V where saturation coverage is approached. In all the solutions, the onset of the signal is near the potential of zero charge, PZC. The reported value of PZC for polycrystalline silver in NaClO₄ is -950 mV (ref. 14). Our concentration studies show values of -900 to -1050 mV for 0.2 to 100 mM concentration of NaCl. This negative shift in potential is expected for an electrolyte containing specifically adsorbing anions such as Cl⁻. Additional studies with other electrolytes give similar results.

This study provides further evidence that the SH profile on silver electrodes is dominated by the electric field component of the polarizability and can be used to detect sub-monolayer concentrations of the adsorbed species. Additional work is in progress with the goal of making quantitative measurements of adsorbing ions and molecules at electrode surfaces.

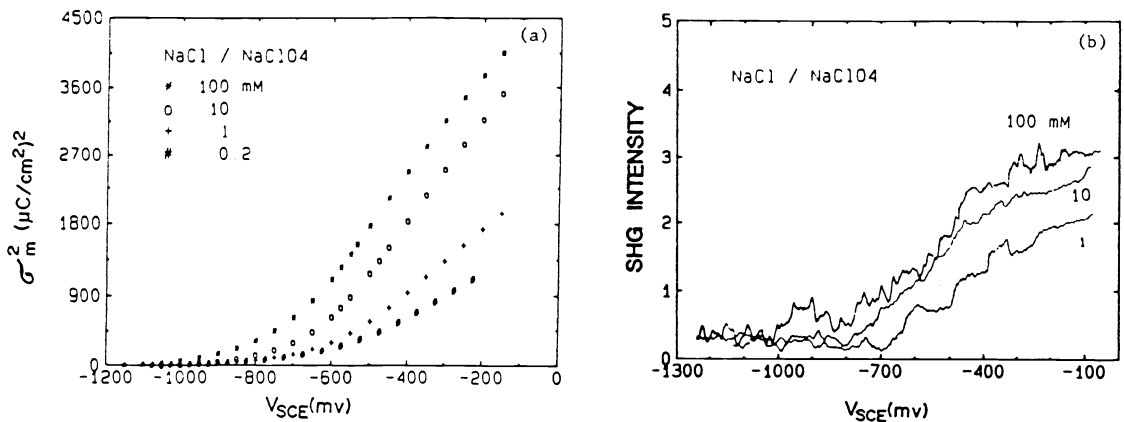


Fig. 3. (a) Potential dependence of the square of the surface charge density for electropolished polycrystalline silver in NaCl-NaClO₄ mixtures at ionic strength 0.5 and chloride ion concentration of 0.2, 1, 10 and 100 mM. (b) Potential dependence of the SHG signal for the same electrochemical system.

SHG as a probe of electrode surface structure

Surface structural information may be obtained through an appropriate selection of excitation polarization and second harmonic field polarization. This approach has been previously exploited to obtain structural information on various semiconductors in air and in UHV by several workers (refs. 15-18). The results described here demonstrate that similar measurements can be obtained at the solid-liquid junction.

A fixed polarization of the incident and reflected beams is selected and the crystal face is rotated about its surface normal. As the crystal is rotated, the second harmonic intensity is dictated by the symmetry of the crystal. Figure 4 shows the variation in the s-polarized SH intensity as a function of angle of rotation for a Ag(111) electrode immersed in water with p-polarized incident light. The result is a sixfold symmetric pattern, consistent with the surface having 3m symmetry. This pattern disappears as the surface is electrochemically roughened, forming an isotropic polycrystalline face. Thus, these measurements, the first of their kind, demonstrate the single crystal nature of the electrode surface in solution.

The SH signal measured is a result of both surface and bulk contributions. At the surface where there is no inversion symmetry and electric dipole terms are allowed, the nonlinear polarization is written:

$$\vec{P}_S(2\omega) = \overset{\leftrightarrow}{\chi}^{(2)} : \vec{E}(\omega)\vec{E}(\omega) \quad (3)$$

The symmetry of the surface is reflected in the form of the nonlinear susceptibility tensor, $\overset{\leftrightarrow}{\chi}^{(2)}$.

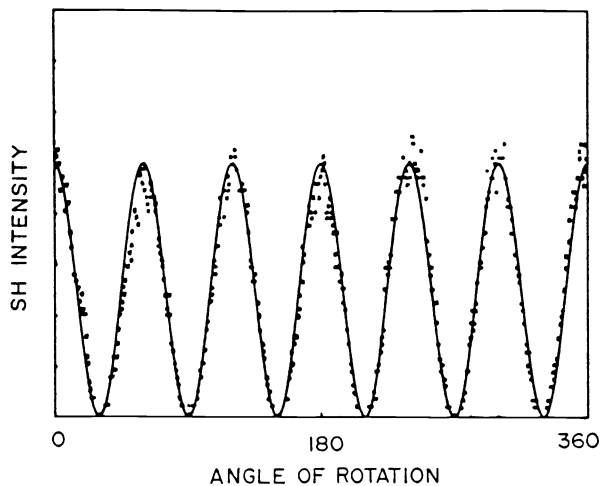


Fig. 4. S-polarized second harmonic intensity as a function of angle of rotation for a Ag(111) electrode in water with p-polarized illumination. The solid curve is a fit to the data (points) using Eq. 5.

In the bulk of a centrosymmetric medium, there are non-local, magnetic-dipole and electric-quadrupole, contributions. For a cubic medium such as silver, the bulk nonlinear polarization may be written:

$$P_{B,i}(2\omega) = (\delta - \beta - 2\gamma)(\vec{E}(\omega) \cdot \vec{\nabla})E_i(\omega) + \beta E_i(\omega)(\vec{\nabla} \cdot \vec{E}(\omega)) \\ + \gamma \nabla_i [\vec{E}(\omega) \cdot \vec{E}(\omega)] + \zeta E_i(\omega) \nabla_i E_i(\omega) \quad (4)$$

where δ , β , γ and ζ are constants which describe the nonlinear response of the material. The first three terms give rise to an isotropic contribution, while the last term gives rise to an anisotropic contribution that is determined by the crystal symmetry.

From the expressions above, a solution may be calculated for the s-polarized component of the SH electric field for p-polarized excitation on a (111) surface (ref. 15):

$$E_S^{(111)} \propto (\chi_{\xi\xi\xi}^{(2)} + a\zeta)(\cos^3\theta - 3\cos\theta\sin^2\theta) \quad (5)$$

where θ is the angle of rotation of the ξ axis of the crystal with respect to the normal of the plane of incident radiation, and $\chi_{\xi\xi\xi}^{(2)}$ is the anisotropic element in the nonlinear susceptibility tensor for the (111) surface. The constant a is dependent on the input beam geometry, but independent of sample rotation. This expression, when squared to yield the SH intensity, is in good agreement with the data (Fig. 4). We have also measured the p-polarized SH intensity for p-polarized excitation in a complementary study. The results provide additional information about the isotropic components of the polarizability and will be reported elsewhere (ref. 19).

In order to characterize a surface completely by this method, the SH signal from the bulk must be distinguished from the surface SH signal. In the work on Si(111) and Si(100) crystals, it was found that the surface and the bulk make comparable contributions (ref. 15). Experiments are currently underway in this laboratory which exploit various electrochemical processes to mask or enhance the surface contribution to the SH signal in order to determine the relative magnitudes of the surface and bulk terms.

SHG measurements from chalcogenide materials

Second harmonic generation from the surface of isotropic Se films is readily observed using the picosecond laser system. The measured signal at 532 nm is monochromatic. Photoinduced carrier production is minimized since the bandgap of a-Se is 2 eV, well above the energy of the fundamental beam (ref. 20). Furthermore, by employing a subbandgap probe, these experiments successfully avoid the broad infrared photoluminescence which has been observed from a-Se using visible photoexcitation at low temperature (ref. 21). Although a-Se has been widely used in various photoassisted applications, the current understanding of the voltage dependent carrier dynamics controlling its usefulness is in an elementary state. The ease with which the signal is obtained, the lack of interfering luminescence and the known sensitivity of SHG to electric field effects make SHG a potentially ideal probe of kinetic processes in a-Se.

The SH signal from these films can be enhanced by controlling the thickness of the film. We observe that SHG increases with sample thickness and attains a maximum for films of bulk thickness (Fig. 5). Similar behavior was observed by Wokaun *et al.* (ref. 22) when SHG was monitored from gold island films of 0 to 200 Å thickness. The authors attribute the increase to the launching of extended surface plasmons.

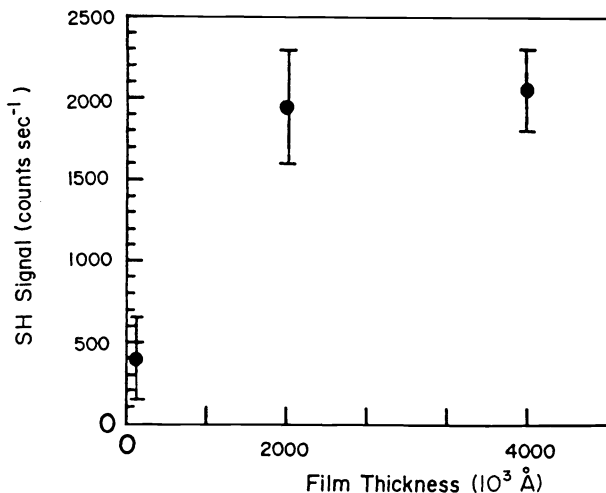


Fig. 5. Depth dependence of SH signal from amorphous selenium films.

Two transition metal dichalcogenides WSe_2 and $ZrSe_2$ have also been investigated under ambient conditions. SH light at 532 nm is readily observed from the surface and is free of potentially interfering luminescence. Our interest in these materials is that they have several unique properties which make them ideal model compounds for studying photoinduced processes at solid/liquid interfaces by nonlinear optical methods. One particularly important property is that a single crystal, oxide free surface is easily prepared by peeling the top layer of the material from the bulk sample (ref. 23). No surface damage or accompanying photoluminescence is observed at the low laser fluence used here. Photoexcitation with visible light (refs. 23,24) of many of the dichalcogenides results in efficient photocarrier production. Studies are now in progress to investigate time dependent phenomena in these dichalcogenides as well as the selenium films.

CONCLUSIONS

We have demonstrated a few examples of the diverse applications of SHG to the measurement of the properties of solid/liquid and solid/air junctions. Although current understanding of this technique is far from complete, second harmonic generation clearly has the potential to be a valuable interfacial probe for general use.

Acknowledgements

We gratefully acknowledge the National Science Foundation (NSF #8513008 and CHE #8451346), the Petroleum Research Fund of the American Chemical Society (PRF-AC516905), and the Department of Energy (DEFG06-86ER45273) for their respective support of this work. Support from the Alfred P. Sloan Foundation is appreciated by GLR. We also thank M. Crawford and B. A. Parkinson for the semiconductors and helpful discussions.

REFERENCES

1. N. Bloembergen, R.K. Chang, S.S. Jha, and C.H. Lee, *Phys. Rev.*, **174**, 813-822 (1968).
2. Y.R. Shen, *J. Vac. Soc. Technol. B*, **3**, 1464-1466 (1985).
3. T.F. Heinz, M.M.T. Loy, and W.A. Thompson, *J. Vac. Sci. Technol. B*, **3**, 1467-1470 (1985).
4. J.M. Hicks, K. Kemnitz, K.B. Eisenthal and T.F. Heinz, *J. Phys. Chem.*, **90**, 560-562 (1986).
5. G.L. Richmond, *Langmuir*, **2**, 132-139 (1986).
6. G.L. Richmond, *Chem. Phys. Lett.*, **110**, 571-575 (1984).
7. R.M. Corn, M. Romagnoli, M.D. Levenson, and M.R. Philpott, *Chem. Phys. Lett.*, **106**, 30-35 (1984); *J. Chem. Phys.*, **81**, 4127-4132 (1984).
8. R. Sonnenfield and B.C. Schardt, *Appl. Phys. Lett.*, **49**, 1172-1174 (1986).
9. J.T. Hupp, D. Larkin, and M.J. Weaver, *Surf. Sci.*, **125**, 429-451 (1983).
10. For reviews: Y.R. Shen in "Chemistry and Structure at Interfaces", R.B. Hall and A.B. Ellis, eds. (VCH Publishers, Deerfield Beach, FL, 1986), Chapter 4.
11. G.L. Richmond, *Chem. Phys. Lett.*, **106**, 26-29 (1984); **113**, 359-363 (1985).
12. C.H. Lee, R. K. Chang, and N. Bloembergen, *Phys. Rev. Lett.*, **18**, 167-170 (1967).
13. G.L. Richmond, H.M. Rojhtantalab, J.M. Robinson, and V.L. Shannon, *J. Opt. Soc. Am. B*, **4** (1987), in press.
14. D.I. Leikis, K.V. Rybalka, E.S. Sevastyanov, and A.N. Frumkin, *J. Electroanal. Chem.*, **46**, 161-169 (1973).
15. H.W.K. Tom, T.F. Heinz, and Y.R. Shen, *Phys. Rev. Lett.*, **51**, 1983-1986 (1983).
16. J.A. Litwin, J.E. Sipe, and H.M. van Driel, *Phys. Rev. B*, **31**, 5543-5546 (1985).
17. D. Guidotti, T.A. Driscoll, and H.J. Gerritsen, *Solid State Comm.*, **46**, 337-340 (1983).
18. T.A. Driscoll and D. Guidotti, *Phys. Rev. B*, **28**, 1171-1173 (1983).
19. V.L. Shannon, D.A. Koos, and G.L. Richmond, in preparation.
20. A.K. Bhatnagar and K. Venugopala Reddy, *J. Non-Cryst. Solids*, **76**, 409-411 (1985).
21. R.A. Street, T.M. Searle and I.G. Austin, *Philos. Mag.*, **29**, 1157-1169 (1974).
22. A. Wokaun, J.G. Bergman, J.P. Heritage, A.M. Glass, P.F. Liao and D.H. Olson, *Phys. Rev. B*, **24**, 849-856 (1981).
23. H. Tributsch, *Discuss. Faraday Soc.*, **70**, 189-205 (1980).
24. K.K. Kam and B.A. Parkinson, *J. Phys. Chem.*, **86**, 463-467 (1982).